Stochastic Resonance in a Neuronal Network from Mammalian Brain

Bruce J. Gluckman,[1,2] Theoden I. Netoff,[2,3] Emily J. Neel,[2] William L. Ditto,[4] Mark L. Spano,[1] and Steven J. Schiff[2,3]
[1]*Naval Surface Warfare Center, Silver Spring, Maryland 20903*
[2]*Department of Neurosurgery, Children's National Medical Center and The George Washington University School of Medicine, Washington, D.C. 20010*
[3]*Program in Neuroscience, The George Washington University, Washington, D.C. 20052*
[4]*School of Physics, Georgia Institute of Technology, Atlanta, Georgia 30332*
(Received 24 June 1996)

Stochastic resonance, a nonlinear phenomenon in which random noise optimizes a system's response to a signal, has been postulated to provide a role for noise in information processing in the brain. In these experiments, a time varying electric field was used to deliver both signal and noise directly to a network of neurons from mammalian brain. As the magnitude of the stochastic component of the field was increased, resonance was observed in the response of the neuronal network to a weak periodic signal. This is the first demonstration of stochastic resonance in neuronal networks from the brain. [S0031-9007(96)01583-9]

PACS numbers: 87.22.Jb, 02.50.Ey, 05.40.+j, 87.50.–a

The brain is a noisy processor, and the idea that the brain might make use of such noise to enhance information processing is not new [1]. In stochastic resonance (SR), the response of a nonlinear system to an otherwise subthreshold signal is optimized with the addition of noise. Since its proposal as a mechanism for amplifying the effects of the Earth's small periodic orbital variations by random meteorological fluctuations leading to ice age periodicity [2], SR has been observed in a diverse range of physical systems [3]. Despite theoretical work predicting that SR might be found in single neurons [4] and neuronal networks [5,6], and experimental evidence suggestive of SR from interspike interval histograms (ISIH) [7], there has been no experimental confirmation in the brain. SR has previously been observed in the activity of single mechanoreceptive sensory neurons from crayfish [8], rat skin [9], and from single interneurons from cricket abdominal ganglia [10]. Each of these previous demonstrations of SR involved the processing of mechanosensory information, when signal and noise were encoded into environmental pressure fluctuations.

Adjusting the noise of neurons directly has been difficult. In the crayfish two approaches have been taken for optimizing detection sensitivity to pressure fluctuations. Raising the temperature failed to show optimization as a function of noise level [11], while raising the light level on the caudal photoreceptor has been successful [12]. Nevertheless, because of the technical difficulty of delivering signal and noise directly to neurons, the experimental study of SR in mammalian brain has remained an intractable problem.

In recent work we demonstrated that an electric field could be used to either suppress or enhance epileptiform activity in mammalian brain slices [13]. The effect of an imposed electric field on neurons has been worked out in detail, and it is well known that the amplitude of an electric field required to modulate the action potential timing of an actively firing neuron is much less than that required to initiate an action potential in a neuron from rest [14]. The physics can be understood by considering a field aligned parallel to the axis between the dendrites, where signals come in from other neurons, and the soma, where these signals are translated into action potentials. The field induces ionic currents both inside and outside the neurons, but the cell membranes act as containers (albeit leaky ones) causing charge to build up and thereby changing the transmembrane potential at the somata. The result on each neuron is a shift in the effective threshold for action potential initiation, and therefore a modulated response to incoming signals. Because the electric field interacts with neurons even at magnitudes insufficient to trigger action potentials, it provides a means to introduce a subthreshold signal into an entire network of neurons to probe for SR.

A schematic of the experimental setup is shown in Fig. 1(a). Longitudinally or transversely cut hippocampal slices (400 μm thick) from rat temporal lobe [15] were placed in the center of a field produced by parallel nonpolarizing Ag-AgCl electrode plates submerged in the perfusate. The neural layers of the slice, which are visually identifiable, are oriented with respect to the field. The potential between the plates was set by a computer generated signal applied through an isolation amplifier. The resulting field in the chamber, and within a slice, was measured and calibrated to the potential applied to the plates [Figs. 1(b) and 1(c)]. The field is quite uniform in the central region of the chamber where the slices are placed, and is proportional to the potential applied to the plates over the range of amplitudes and frequencies used in these experiments.

Hippocampal slices in a high (8.5 mM) potassium perfusate, as used in these experiments, demonstrate increased neuronal synchrony and spontaneous *ensemble* activity [16] in which large populations of the main excitatory

 0031-9007/96/77(19)/4098(4)$10.00

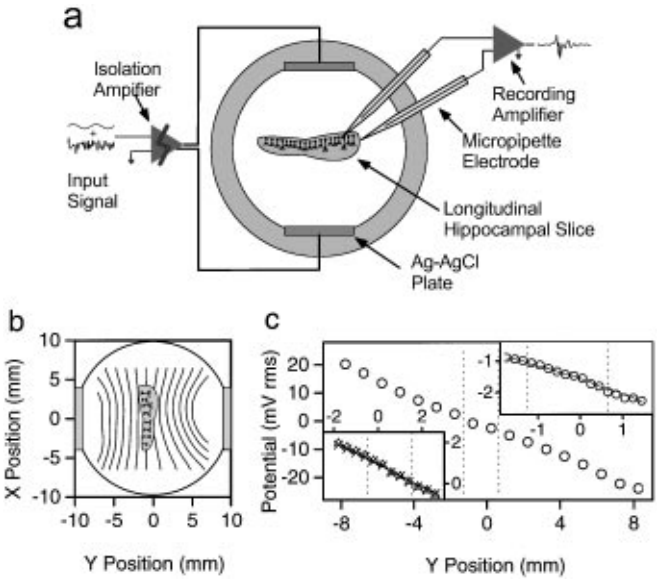

FIG. 1. (a) Schematic of perfusion chamber as viewed from above. The hippocampal slice [15] rests just below the upper surface of the bath. An electric field is imposed by a potential difference between parallel Ag-AgCl plates submerged in the bath. (b) and (c) Mappings of electrical potential within chamber with a 100 mV rms sinusoidal potential applied to plates (frequency $f = 60$ Hz, unless specified). (b) Isopotential lines (2.5 mV rms apart) derived from 1 mm spaced measurements with a longitudinal slice in the chamber. (c) Potential (rms) within chamber with and without a slice present (−− indicates slice boundary). Main graph: Potential ○ averaged over $-3 < X < 3$ mm [axes as in (b)]. Upper inset: Potential ○ with slice, – without slice. Lower inset: Potential △ with slice $f = 65$ Hz, × with slice $f = 5$ Hz, – without slice $f = 35$ Hz. Measurements made 50 μm from surface of slice, similar results observed at depth 100 μm. The field within the slice is fairly uniform, nearly identical to the field within the chamber, and proportional to the applied potential for the range of frequencies used in this experiment.

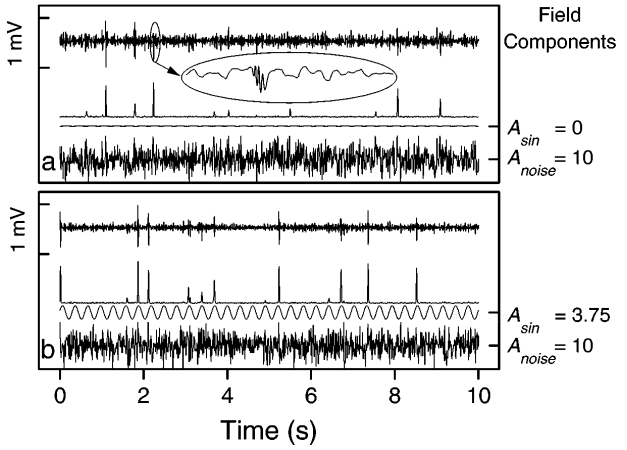

FIG. 2. Activity in CA1 layer of a longitudinal slice with imposed electric field. In each panel: First trace is extracellular potential (analog filtered between 200–1000 Hz). Inset in (a): expanded view of a burst, identified by 250 Hz oscillation. Second trace is processed signal [18] used to identify bursts. Lower traces are periodic and stochastic components of imposed field. With only a periodic signal (not shown) no events are observed. With just noise input (a), events occur randomly in time. With both sinusoid and noise (b), events occur primarily near the positive peak of the sine wave.

neurons that define the output of these networks burst fire at the same time. Such activity is an emergent property of the network, and is observed as large stereotyped extracellular potential changes in the cell body layers (CA1 or CA3 [17]), but not clearly seen at the single cell level.

In order to detect these synchronous population events (bursts), the potential within the cell body layer was measured with an extracellular electrode, referenced to an electrode in the bath on nearly the same isopotential of the imposed field. This configuration minimized measurement artifacts from the imposed field. Because some remnant of the input signal leaked into the recording, the input signals were carefully chosen to ensure that neuronal bursts could be differentiated from stimulus artifact. Bursts typically last 10–30 ms, occur as frequently as a few Hz, and can be identified from characteristic oscillations near 250 Hz [see Fig. 2(a) inset]. We therefore chose an input signal composed of a sinusoid with frequency $f_0 < 4$ Hz (amplitude $A_{\rm sin}$) and a noise signal with a high frequency cutoff $f_0 \ll f_{\rm nmax} \ll 250$ Hz. The noise was Gaussian distributed in amplitude with a root mean square (rms) width of $A_{\rm noise}$.

Responses of a typical network to different inputs are illustrated in Fig. 2. In both panels, the upper two traces are digitized recordings of network activity (raw and processed [18]), and the lower traces depict the periodic and stochastic components of the imposed field. No burst events were observed for this network for a sinusoidal signal (frequency $f_0 = 3.3$ Hz) with amplitude less than $A_{\rm sin} \simeq 7$ mV/mm. With a pure noise input ($A_{\rm noise} = 10$ mV/mm, $f_{\rm nmax} = 26$ Hz), randomly occurring bursts were observed [Fig. 2(a)]. With both noise and subthreshold sinusoid ($A_{\rm sin} = 3.75$ mV/mm) [Fig. 2(b)], bursts occurred preferentially near the maxima of the sinusoid. This is the essence of SR—the behavior of a noise driven system can be modulated by the introduction of an otherwise subthreshold signal.

One way to quantify this modulation is to measure the probability of a burst occurring as a function of the phase ϕ of the sinusoidal field $P_{\rm burst}(\phi)$. This burst probability density (BPD) is shown in Fig. 3(A) for various combinations of sinusoid and noise. The phase ϕ is indicated by the sinusoid drawn at the center of the column. The BPD is normalized so that its integral is the mean burst rate per cycle of the drive. With $A_{\rm sin} = 0$ and moderate $A_{\rm noise}$ (a) the bursts occur randomly with respect to ϕ. In contrast, with the subthreshold sinusoid added to the noise, the BPD is a peaked function of ϕ (b). As a function of increasing $A_{\rm noise}$, the peak becomes taller, corresponding to an increase in the average burst rate, and broader, corresponding to a decrease in the

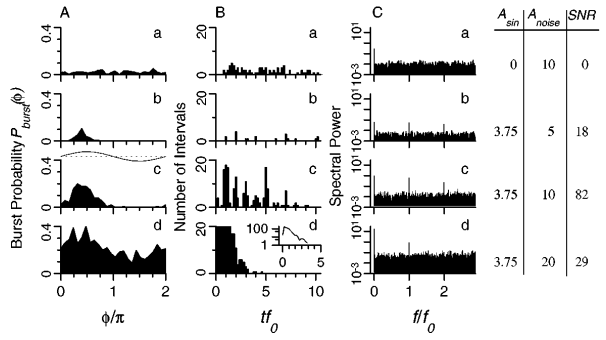

FIG. 3. (A) Burst probability densities (BPD) $P_{\mathrm{burst}}(\phi)$, (B) interspike interval histograms (ISIH), and (C) power spectral densities (PSD) from the same experiment as in Fig. 2 ($f_0 =$ 3.3 Hz, $f_{\mathrm{nmax}} = 26$ Hz). Field amplitudes (in mV/mm) and signal to noise ratio (SNR) [22] given at right. BPD computed as function of phase ϕ of the sinusoidal signal; phase is indicated by the tracing $\sin(\phi)$ between (b) and (c). ISIH's based on events within 170 s measurements. Data from (Bd) shown on logarithmic scale in inset. With $A_{\mathrm{noise}} = 0$ and $A_{\mathrm{sin}} = 0$ or 3.75 (not shown) no bursts were observed, and all three measures were zero. With just noise input (top row), no modulation is observed in either the BPD or the ISIH and no frequency dominates the PSD. Combinations of noise and subthreshold sinusoid yield a peaked structure in the BPD, organization in the ISIH at multiples of the drive period, and a peak in the PSD at $f/f_0 = 1$.

synchronization of single burst events with a particular phase of the sinusoid (c) and (d).

This periodic modulation can also be detected from the distribution of interevent intervals [19], a measure with a long tradition in the characterization of neuronal dynamics [20]. ISIH are shown for our data in Fig. 3(B). With just noise (a), the ISIH is featureless. In contrast, with a small amount of noise and a subthreshold periodic signal (b), nearly all of the intervals observed occur at integer multiples of the drive period. As the noise level is increased (c) these peaks become wider and the envelope defining their amplitudes appears more exponential (inset of d). The envelope's decay time decreases with increasing noise. For the highest noise level shown, no peaks are distinguishable from the ISIH, although modulation is still observed in $P_{\mathrm{burst}}(\phi)$.

The standard method of quantifying the resonance between a periodic input and the system's response is to compare its spectral power at the input frequency to the power observed at other frequencies. Example power spectral densities (PSD) [21] are shown in Fig. 3(C). For purely randomly occurring bursts, as are observed with noise input alone, spectral power is evenly distributed over frequency (a). With the combination of both periodic and stochastic inputs, a peak is observed at f_0 and at its harmonics, $f/f_0 = \{1, 2, \ldots\}$. The power at these frequencies could be derived from an integral over $P_{\mathrm{burst}}(\phi)$. As a function of the noise component of the input, the amplitudes of both the peak at f_0 and of the background change. The ratio of these amplitudes, the signal to noise ratio (SNR) [22], is maximal at an intermediate input noise level.

The SNR as a function of A_{noise}, with constant A_{sin}, is shown in Fig. 4(a) for the same experiment as Figs. 2 and 3. A series of these optimization curves, corresponding to different values of A_{sin}, are shown in 4(b) from a different experiment. In each case, a maximum is observed in the SNR at intermediate noise levels. Also, as would be expected, as A_{sin} is increased, the maximal value of SNR increases and occurs at lower noise levels. Experiments were performed on 12 slices from 9 rats. When analyzed as in Fig. 4, SR was documented in 9 experiments (5 longitudinal and 2 transverse slices measured from CA1 layer; 2 transverse slices measured from CA3 layer).

In many of these experiments the network demonstrated no burst-firing activity without an imposed field, and a completely subthreshold A_{sin} could be chosen [as in Fig. 2(a)]. In this case SNR $= 0$ at $A_{\mathrm{noise}} = 0$. In contrast, three of the networks studied exhibited burst events without the introduction of a field. In these cases, sinusoidal signals that did not excite new bursts still modulated the timing of the bursts and could be detected from the PSD. Although SNR > 0 at $A_{\mathrm{noise}} =$ 0, optimization was still observed with additional noise.

In contrast to previous biological experiments, we have shown SR in the behavior of a network of neurons from mammalian brain. Although SR for individual nonlinear elements is fairly well understood, much less is known about the effects of different types of noise and coupling in arrays or networks of devices. Noise in an array of elements can be either local, where the noise sources for each element are independent and uncorrelated [6,23], or global, where the noise is uniform across the array [24,25]. Our experiments correspond to global noise,

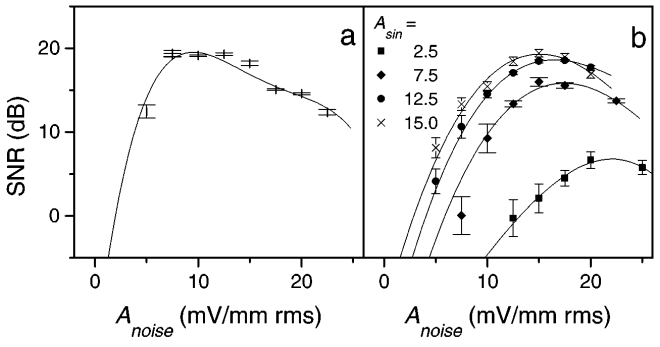

FIG. 4. Signal to noise ratio (SNR) in decibels [$10 \log_{10}$(SNR)] as function of A_{noise} (a) for experiment in Figs. 2 and 3 ($f_0 = 3.3$ Hz, $f_{\mathrm{nmax}} = 26$ Hz) and (b) a different slice ($f_0 =$ 3.09 Hz, $f_{\mathrm{nmax}} = 20$ Hz). In both cases, SNR(0) $= 0$. Solid lines provided to guide the eye. In (b) a family of measured optimization curves are shown for varying A_{sin}. As A_{sin} is increased, the maximum value of SNR increases and occurs at lower A_{noise}. Error bars estimated from rms distribution of multiple measurements where possible, or proportional to counting error (inverse square root of number of events).

where the random fluctuations in the external electric field produced correlated noise at each element in the neural array. Although one might anticipate that global noise would make the detection of SR more difficult in an array [25], this did not prove to be an impediment to SR identification in these experiments.

Whether or not environmental electromagnetic radiation could have significant health effects [26], and whether SR may play a role [3,27], is controversial. Neuronal modulation, in the presence of noise, was shown in Figs. 2–4 at field strengths weaker than previous reports [14]. Our experiments suggest that SR could be a mechanism for amplification of weak electrical field effects on the brain. We further speculate that SR could enhance effects of weak intrinsic 4–10 Hz hippocampal theta or more widespread 40 Hz gamma oscillations within the brain [28].

Nervous systems, from invertebrates to man, are noisy—membrane potentials fluctuate, membrane channels open and close, and quantal release at synapses is probabilistic. Two hypotheses seem apparent: either nervous systems evolved to include noise within their circuits as an advantage to processing, or, perhaps more palatable, the components that all nervous systems had to use in their evolution were inherently noisy and brains had to make the best of it. Regardless of the teleology involved, the findings presented here show that random noise can enhance the response to a signal within a mammalian neuronal network.

This work was supported by National Institutes of Health (1R29-MH50006-04), United States Office of Naval Research (ONR) (N00014-95-1-013), and The Children's Research Institute.

[1] W. R. Adey, Int. J. Neurosoci. **3**, 271 (1972).
[2] R. Benzi *et al.,* J. Phys. A **14**, L453 (1981).
[3] K. Wiesenfeld and F. Moss, Nature (London) **373**, 33 (1995).
[4] A. Bulsara *et al.,* Biol. Cybernet. **61**, 211 (1989); A. Bulsara *et al.,* J. Theor. Biol. **152**, 531 (1991).
[5] M. Riani and E. Simonotto, Phys. Rev. Lett. **72**, 3120 (1994).
[6] J. J. Collins *et al.,* Nature (London) **376**, 236 (1995).
[7] A. Longtin *et al.,* Phys. Rev. Lett. **67**, 656 (1991); D. R. Chialvo and A. V. Apkarian, J. Stat. Phys. **70**, 375 (1993).
[8] J. Douglass *et al.,* Nature (London) **365**, 337 (1993).
[9] J. J. Collins *et al.,* J. Neurophysiol. **76**, 642 (1996).
[10] J. E. Levin and J. P. Miller, Nature (London) **380**, 165 (1996).
[11] E. Pantezelou *et al.,* Int. J. Bif. Chaos **5**, 101 (1995).
[12] X. Pei *et al.,* J. Neurophysiol. (to be published).
[13] B. J. Gluckman, E. J. Neel, T. I. Netoff, W. L. Ditto, M. L. Spano, and S. J. Schiff, J. Neurophysiol. (to be published).
[14] C. A. Terzuolo *et al.,* PNAS **42**, 687 (1956); J. G. R. Jefferys, J. Physiol. (London) **319**, 143 (1981); C. Y. Chan *et al.,* J. Physiol. (London) **371**, 89 (1986); D. Tranchina *et al.,* Biophys. J. **50**, 1139 (1986); C. Y. Chan *et al.,* J. Physiol. (London) **402**, 751 (1988).
[15] Preparation details in S. J. Schiff *et al.,* Nature (London) **370**, 615 (1994).
[16] P. A. Rutecki *et al.,* J. Neurophysiol. **54**, 1363 (1985); A. F. Traynelis *et al.,* J. Neurophysiol. **59**, 259 (1988).
[17] For anatomy, see A. Brodal, *Neurological Anatomy, Third Edition* (Oxford University Press, New York, 1981).
[18] Digitized signal is bandpass filtered $200 < f < 300$ Hz (characteristic of bursts), rectified, then smoothed (15 ms $\simeq$ burst duration). Bursts then identified by threshold crossings.
[19] T. Zhou *et al.,* Phys Rev. A **42**, 3161 (1990); A. Simon and A. Libchaber, Phys. Rev. Lett. **68**, 3375 (1992); A. Longtin, J. Stat. Phys. **70**, 309 (1993).
[20] H. C. Tuckwell, *Introduction to Theoretical Neurobiology* (Cambridge University Press, Cambridge, 1988), Vol. 2.
[21] PSDs computed from continuous function representing burst times t_n: $V(t) = \sum_n s(t - t_n)$, $s(t)$ chosen so that its transform $\tilde{s}(\omega)$ is known. Then $P(\omega) = |\tilde{s}(\omega) \sum_n e^{-i\omega t_n}|^2$. PSD presented computed with $s(t) = \delta(t)$ ($\tilde{s}_\delta(\omega) = 1$). No significant difference in SNRs found if repeated with Gaussian functions incorporating burst amplitude and duration for $s(t)$.
[22] SNR computed from PSDs as SNR $= (a - b)/b$ where a is amplitude of peak at $f/f_0 = 1$, b is background amplitude averaged over range $0.9 < f/f_0 < 1.1$, excluding the peak.
[23] J. F. Linder *et al.,* Phys. Rev. Lett. **75**, 3 (1995).
[24] S. M. Bezrukov and I. Vodyanoy, Nature (London) **378**, 362 (1995).
[25] M. E. Inchiosa and A. R. Bulsara, Phys. Rev. E **52**, 327 (1995).
[26] L. A. Sagan, *Electric and Magnetic Fields: Invisible Risks?* (Gordon and Breach, Amsterdam, 1996).
[27] I. L. Kruglikov *et al.,* Bioelectromagnetics **15**, 539 (1994).
[28] J. G. R. Jefferys *et al.,*, Trends Neurosci. **19**, 202 (1996); E. R. Kandel *et al., Principles of Neural Science, Third Edition* (Appleton & Lange, Norwalk, 1991).